1965

Wave-tank study of internal waves

Kordek, Walter A.

Monterey, California. Naval Postgraduate School

WAVE-TANK STUDY OF INTERNAL WAVES

WALTER A. KORDEK

WAVE-TANK STUDY OF INTERNAL WAVES

by

Walter A. Kordek

Lieutenant, United States Navy

Submitted in partial fulfillment of
the requirements for the degree of

MASTER OF SCIENCE

United States Naval Postgraduate School
Monterey, California

1 9 6 5

WAVE-TANK STUDY OF INTERNAL WAVES

by

Walter A. Kordek

This work is accepted as fulfilling

the thesis requirements for the degree of

MASTER OF SCIENCE

from the

United States Naval Postgraduate School

ABSTRACT

Internal waves, generated in an approximate two-layer system of miscible fluids by flow over a submarine ridge, were examined. The investigation was conducted in a wave tank 3.0 m long and 0.3 m wide in which total water depth varied between 7.3 cm and 15.2 cm.

To determine visually the interface deformations, the lower saline layer was colored with Rhodamine "B" dye. Neutrally buoyant particles, consisting of a solution of carbon tetrachloride and benzene, were introduced in the vicinity of the pycnocline to indicate particle motion.

Subsequent particle motion and interface deformations were photographed with a 16 mm motion picture camera. Analysis of the film yielded particle trajectories and internal wave characteristics such as wavelength, period, amplitude and phase velocity. The observed motions were compared with those predicted by internal wave theory. Observed phase velocities differed from the theoretical phase velocities in all cases, with a maximum difference in one case of 44 percent of theoretical value. The discrepancies may be due either to the superposition of the observed progressive wave on a standing wave or to the observation of non-conserved wave crests in a dispersive medium. However, observed phase velocities did decrease in magnitude with a decreasing layer density difference as predicted by theory.

LIST OF ILLUSTRATIONS

LIST OF SYMBOLS

h'	depth of upper layer
h	depth of lower layer
T_o	period of wave-generator plate
T_{is}	period of standing internal wave
T_{ip}	period of progressive internal wave
L_{ip}	wave length of progressive wave
L_o	stroke of wave-generator plate
H_i	average vertical oscillation of interface (trough to crest)
ρ'	average density of upper layer
ρ	average density of lower layer
t_w	water temperature
$\triangle \rho$	difference of average densities of two layers
h_B	height of barrier
L_1	length of basin between wave generator and submarine ridge
L_2	length of basin between submarine ridge and wave absorber end-plate
C_{io}	observed phase velocity of internal wave
C_{it}	theoretical phase velocity of internal wave
C	phase velocity
L	wavelength
T	period

1. INTRODUCTION.

1.1 Background.

Fundamental to a systematic investigation of the oceans are mathematical statements of the physical laws involved coupled with an orderly collection of data with which to test these laws. Due to the complexity of the ocean and its vast areas, the collection of sufficient and accurate data for this purpose is no easy task. The requirement for synoptic ocean station observations has generally not been met.

A topic receiving considerable attention in recent years is that of internal waves. Theories have been advanced concerning the environmental factors required for the existence, generation and propagation of internal waves. Analysis of available data has supported many of the theories; however, there remains a constant need for more usable data. With the advent of more sophisticated instrumentation and increased international interest in oceanographic research, as exemplified by the increasing number of trained personnel and research vessels, it is expected that the data requirements will be met in years to come. In the interim the technique of modeling can be used to great advantage to test theories of internal wave motion.

1.2 Advantages of Model Studies.

The major advantage of modeling oceanic processes is the experimental control that can be exercised. Modeling also provides the advantage of economy, both in cost and time.

2. PURPOSE

The objectives of this investigation are:

(1) The design and evaluation of a model tank and wave generator suitable for studying internal waves.

(2) The development of experimental procedures for producing internal waves by causing flow over a submarine ridge model.

(3) To conduct preliminary experiments, collect data, and compare the results with theory.

3. DESCRIPTION OF LABORATORY FACILITIES AND TECHNIQUES.

3.1 Tank.

The facilities of the Oceanography Laboratory at the U. S. Naval Postgraduate School were utilized for this investigation. It should be noted that the wave tank described in this thesis and used in the experiments was originally designed to function as a visual training aid for demonstrating surface wave phenomena.

The tank is rectangular in shape and constructed of aluminum bottom and end plates and plexiglass sides. (The full tank is shown in fig. 1.) It is 3.0 m long, 0.3 m wide and 0.45 m deep with a maximum allowable water depth of 0.3 m due to structural considerations. The tank is supported by a welded aluminum I-beam structure. The full plexiglass sides made observations possible throughout the length of the tank. It is fitted with a bottom drain and valve near one end plate.

3.2 Wave Generator

The wave generator consists of a vertical aluminum plate which oscillates along the longitudinal axis of the tank (fig. 2). There was a 0.3 cm clearance between the face-plate of the generator and the sides and bottom of the tank to prevent metal-to-metal and metal-to-plexiglass abrasion and friction. A gasket to function in the same manner as a piston ring was required to reduce flow by the generator. Foam rubber and rubber "squee-gee" were tried as gasket material but rejected because of excessive friction. Sheet Teflon, 0.15 cm thick, reduced friction but permitted some "flow-by" causing mixing and eddies in the vicinity of the generator. This material was adopted for use.

The wave-generator power system consists of a half-horsepower AC motor and a hydraulic transmission having speed range of 0-1800 rpm input

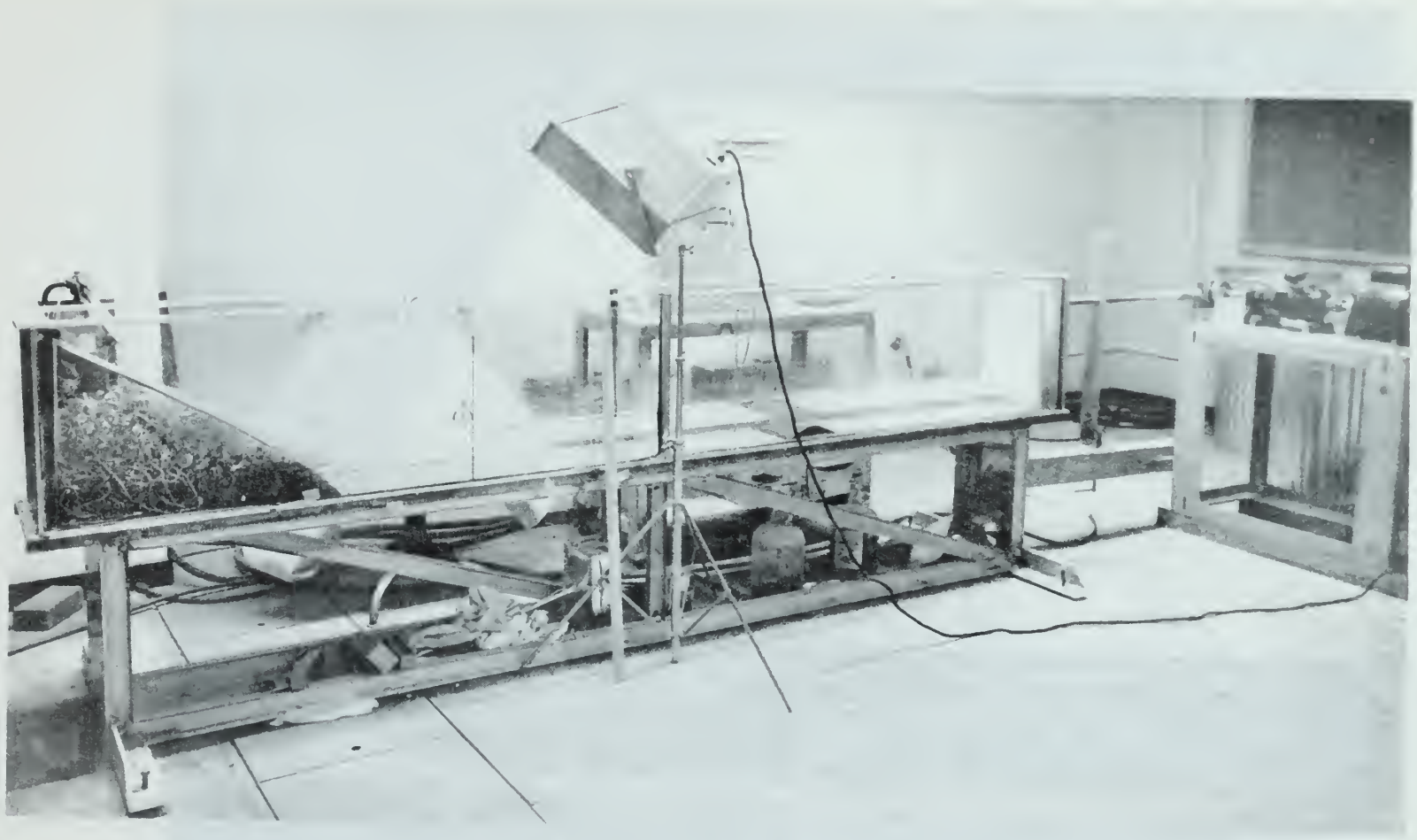

FULL VIEW OF TANK

FIGURE 1

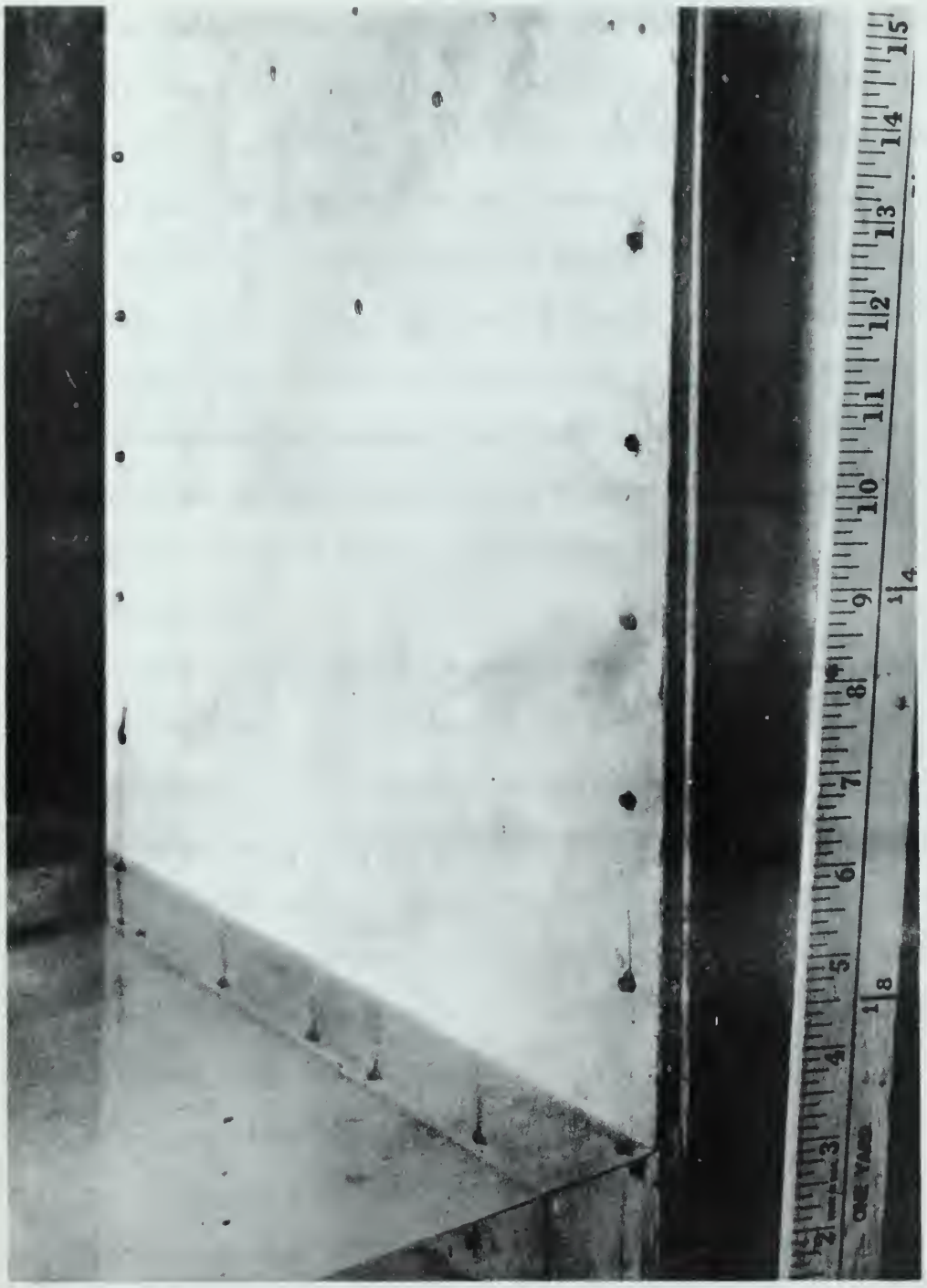

WAVE-GENERATOR PLATE

FIGURE 2

or output (fig. 3). The rotary output of the transmission was transformed to a linear motion to drive the wave generator plate through a crank arrangement shown in fig. 4. The slot at the end of the generator driveshaft permitted the shaft to remain horizontal, thereby eliminating the need for a conventional wrist-pin in the shaft, since the motion of the shaft must be horizontal at the generator plate. The wheel was drilled and tapped at four points, 90 degrees apart, permitting a generator stroke of 3.8, 5.08, 6.35, or 7.62 cm by changing the pin position. The generator shaft enters the tank through a flanged sleeve screwed to the tank endplate. A spreader bar attached to the tank support and the table on which the power assembly was mounted was necessary to prevent "walking" of the table due to motor-induced vibration.

3.3 Wave Absorber.

The wave-absorbing material lies between two aluminum plates which are welded together at right angles and are as wide as the tank (fig. 5). The back plate is 43 cm high and the bottom plate is 61 cm long. The cavity between the plates and the sides of the tank was filled with aluminum shavings and a fine mesh plastic screen drawn tightly over the ends of the plates, forming an angle of 35 degrees with the bottom and completing the enclosure. With a water depth of 15 cm the average absorption distance is 29 cm.

3.4 Submarine Ridge Models.

Two basic types of model were utilized (fig. 6). The first was a 0.3 cm thick aluminum plate cut to the width of the tank. This is shown at the top of fig. 6. The second type consisted of a metal sheet formed over templates, as shown in the lower part of fig. 6. The dimensions were such that the top of the ridge was a sector of a circle with a radius

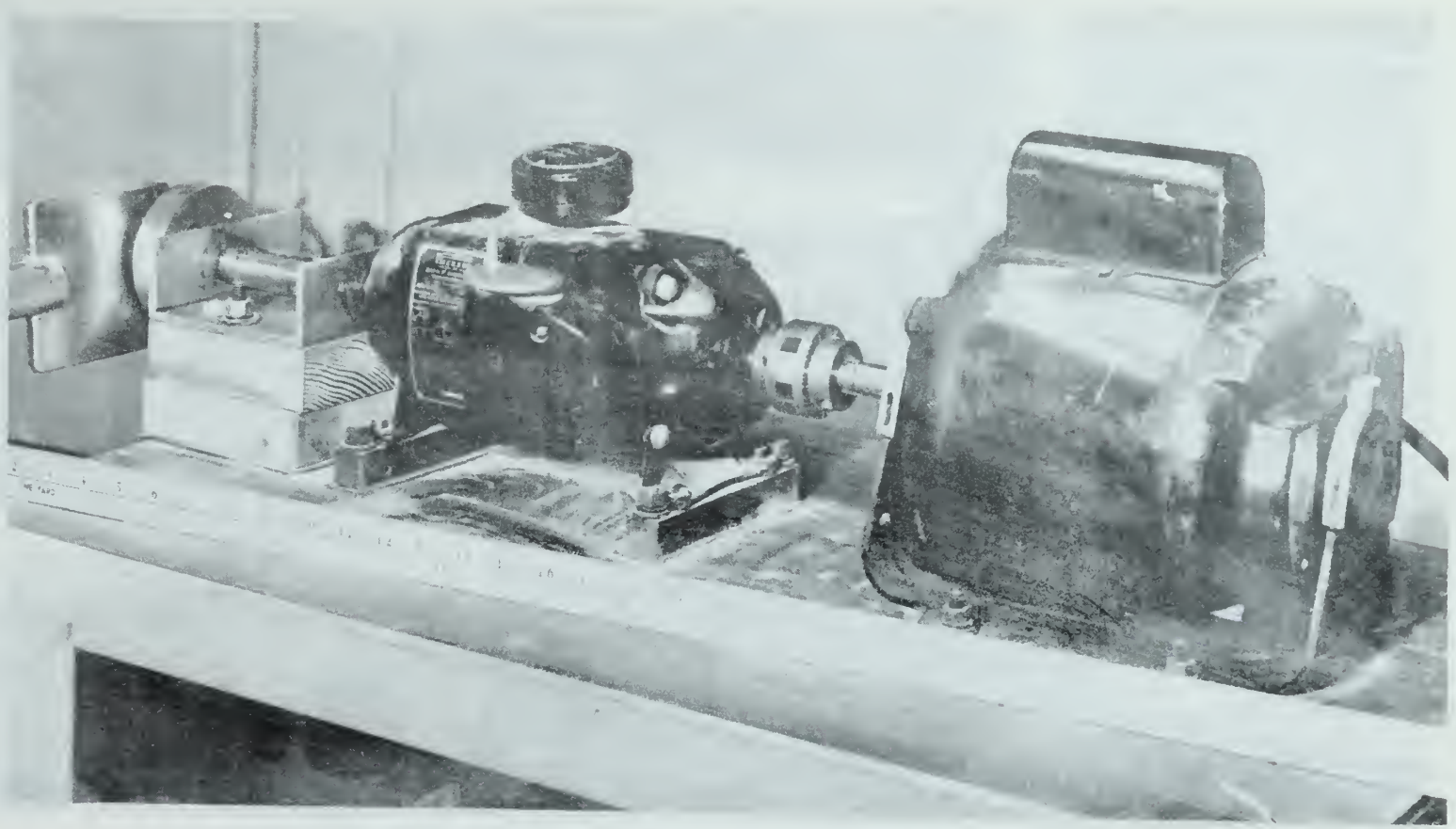

WAVE-GENERATOR POWER ASSEMBLY

FIGURE 3

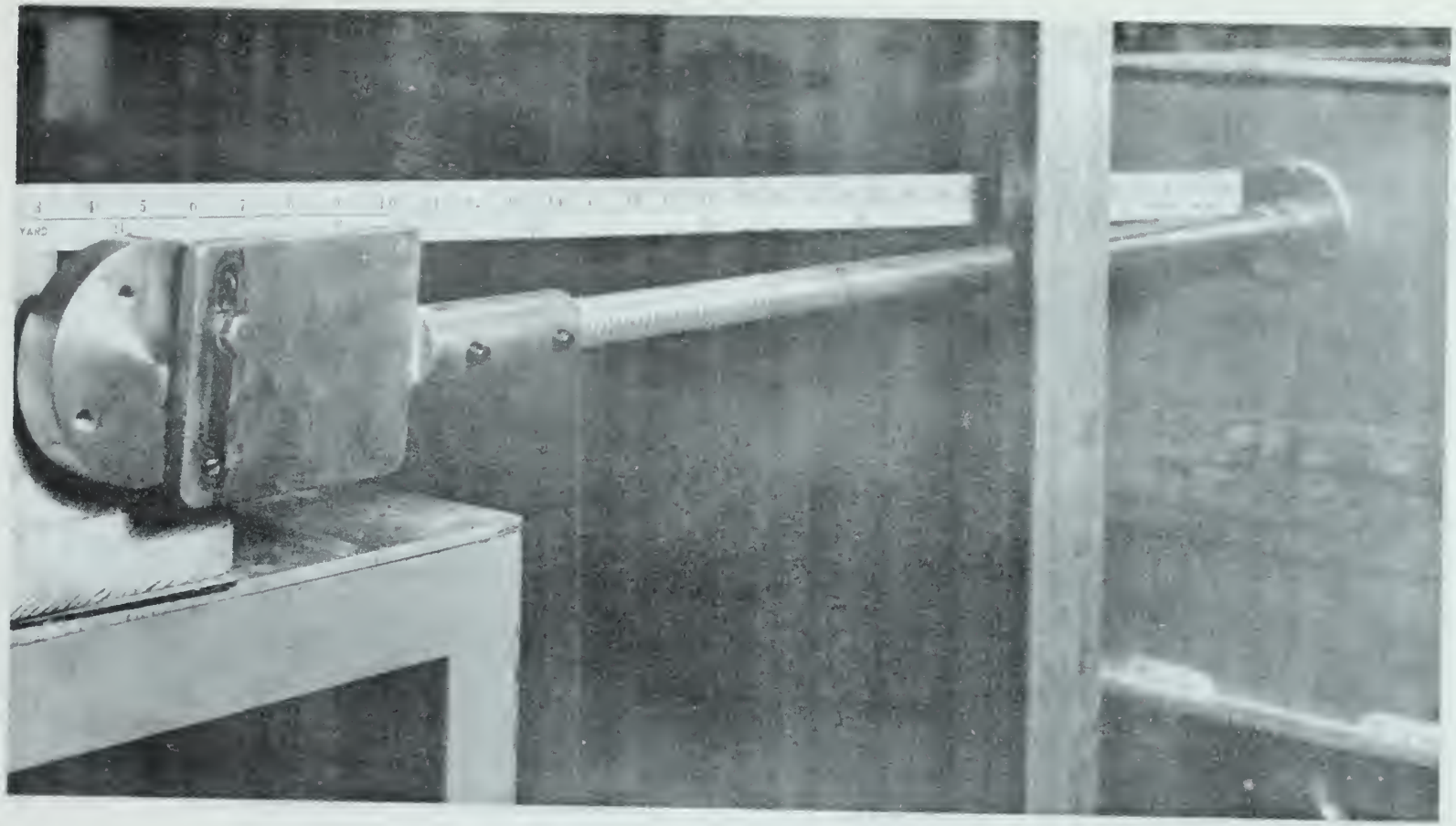

WAVE-GENERATOR DRIVE ASSEMBLY

FIGURE 4

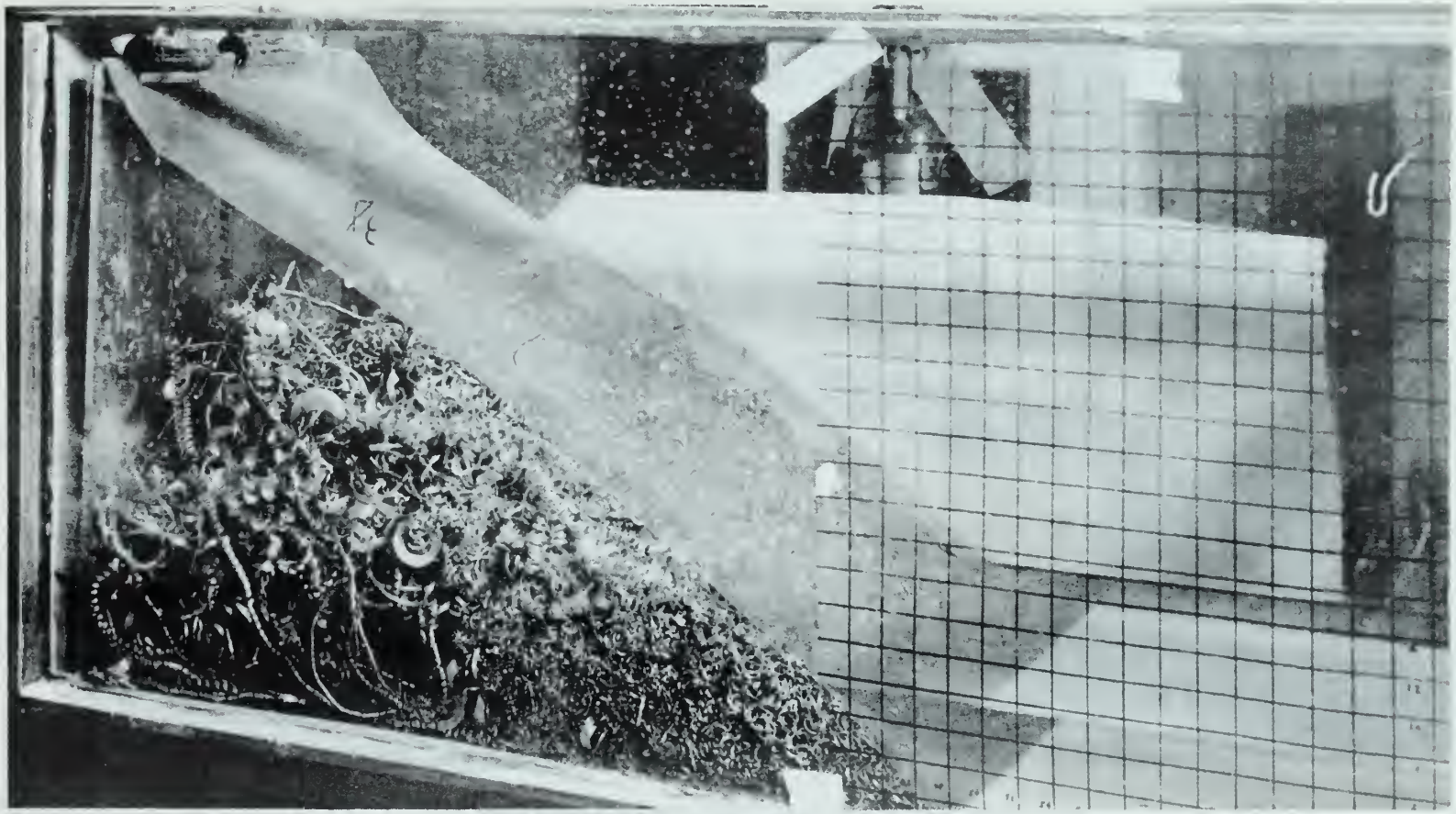

WAVE ABSORBER

FIGURE 5

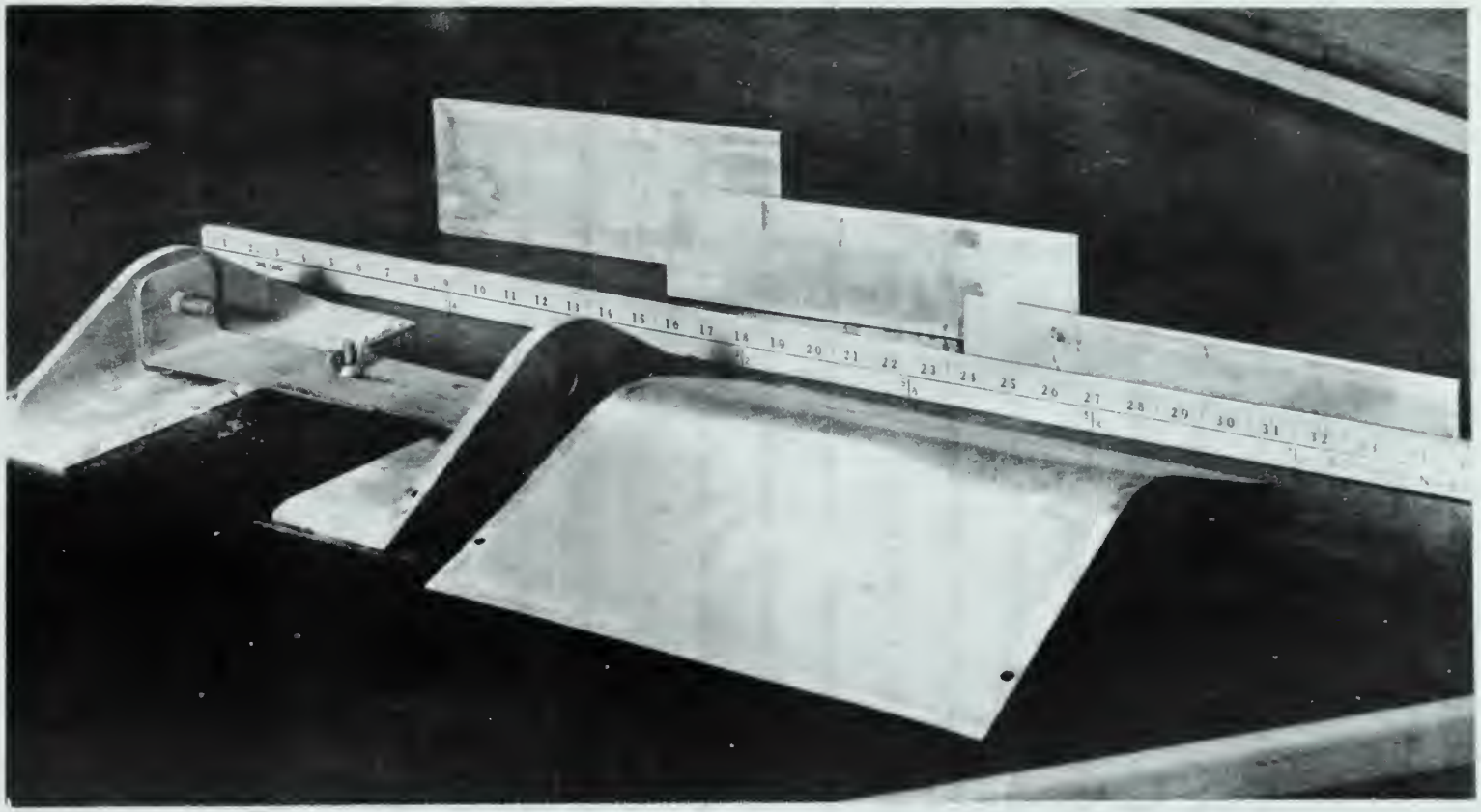

SUBMARINE RIDGE MODELS

FIGURE 6

equal to the height of the ridge and the base equal to four times the height resulting in a slope of 1:2. The sides of the model ridge were sealed with plastic tape. The single-plate model fit snugly against the sides and bottom and needed no sealer.

3.5 Formation of a Two-Layer System.

The fluids used in the two layers were fresh water and a brine solution, which was formed by dissolving rock salt in a vat. These fluids were selected because their miscibility permitted exchange of salt between layers, thus simulating mixing by internal waves as it might occur in the sea. Additionally, the density of the brine was easily controlled and the rock salt required is inexpensive and readily available. Finally, the use of brine added to the simplicity of the problem in that the total salt in the system was conservative. This is a distinct advantage over the use of a temperature difference between layers as described by Cromwell [1], where heat exchange with the environment would give a non-conservative system.

The two-layer system was formed by filling the tank initially with fresh water to depth equal to the desired depth of the upper layer. The siphoning was accomplished by two methods. In one method the brine entered the tank at the bottom drain through a 0.95 cm plastic hose. A small metal plate was placed over the drain to direct the flow horizontally. The valve permitted a controlled rate of flow. By this method a bottom layer with a depth of approximately 8 cm could be introduced in one hour, maintaining a sharp pycnocline.

The second method consisted of placing the outlet of a 0.63 cm rubber tube against the bottom of the tank. The rate of flow was controlled by a "C"-clamp on the hose. The advantage of this method was that it

required no permanent tank installation. The disadvantage is that the rate of flow must be maintained at only about 50 percent of the former method without excessive mixing at the pycnocline.

The brine solution was colored with Rhodamine "B" dye prior to siphoning into the tank. Thirty drops of a 40 percent dye, 60 percent acetic acid solution per 25 gallons of brine yielded the best results. This quantity permitted discrimination of the internal wave form on black and white film while providing sufficient translucence to observe particles of contrasting fluid later introduced.

3.6 Water Sampling and Density Determination.

Water samples were withdrawn with a 30 cc syringe using a 10 cm long needle and a 0.24 cm diameter brass rod 50 cm long (fig. 7). The inlet depth for the needle was determined by taping the rod to the syringe and sliding the syringe along the rod until the desired distance between the bottom of rod and the needle inlet was obtained. Thus when the tip of the rod was held firmly against the bottom of the tank, the sample depth was known.

Two methods of density determination were evaluated. The first method utilized a Bisset-Berman Corporation, Model 621, portable salinometer. Use of this method proved to be a lengthy process with a resultant accuracy in excess of that required for the experiments. The second method utilizing Kahlsico salinity hydrometers was adopted for use in the investigation. The hydrometer method offered the advantages of simplicity of operation while providing sufficient accuracy for the purpose of the investigation. The technique consisted simply of placing the water sample in a 3.8 cm diameter glass cylinder, inserting the hydrometer, which is graduated in units of salinity, and recording the salinity. A

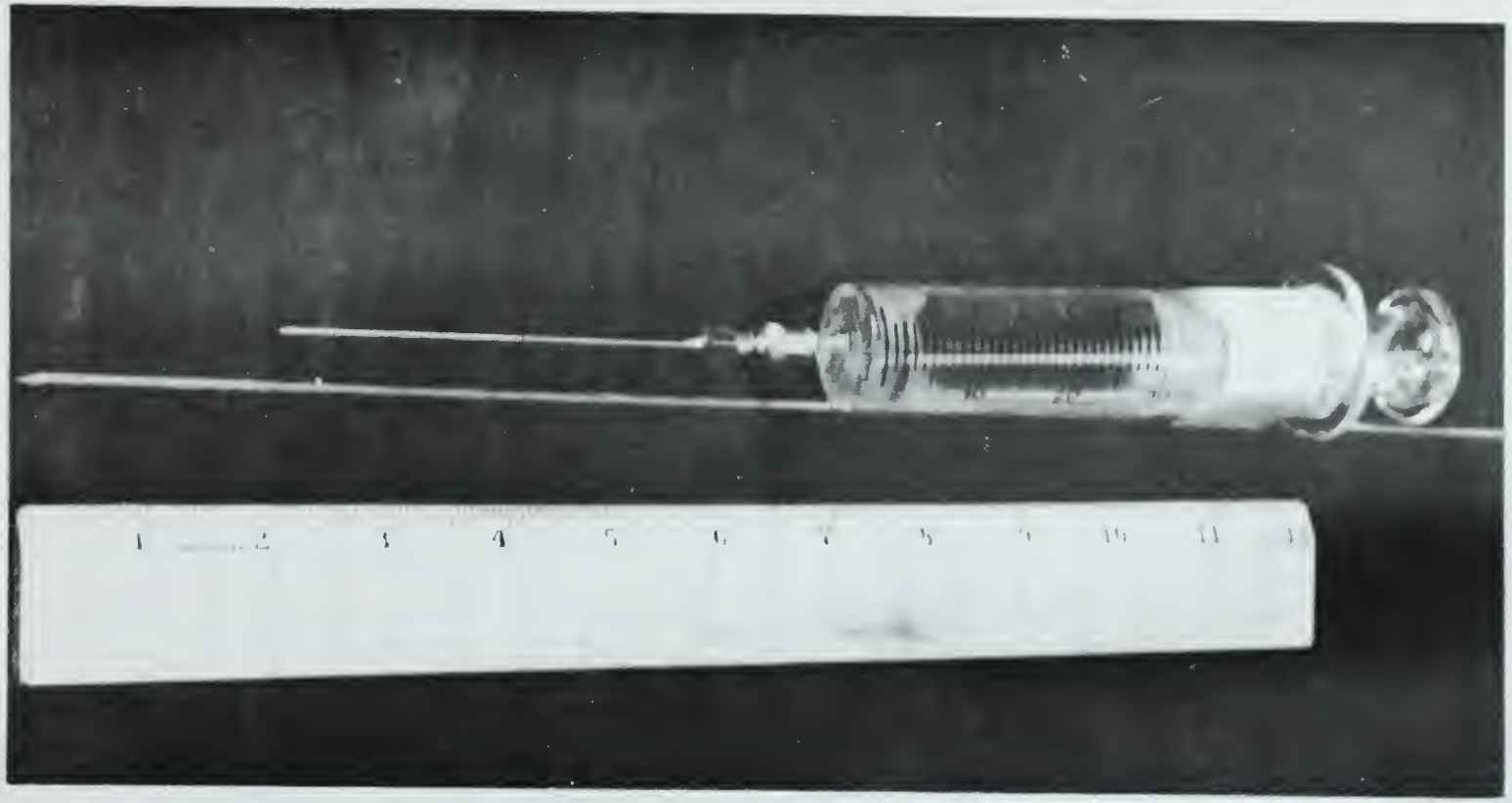

WATER SAMPLING SYRINGE

FIGURE 7

water sample volume of approximately 90 cc was required to float the hydrometer bulb. Corrections were applied for temperature variation and the corrected salinity was then converted to density by use of tables provided with the hydrometers.

3.7 Formation and Introduction of Neutrally Buoyant Particles.

Carbon tetrachloride and benzene were combined in solution such that the resulting density was approximately 1.025 grams per cubic centimeter. A drop of this solution was inserted into the upper layer of the two-layer system with an eye dropper and its motion observed. The particle either settled to the bottom, rose to the surface, or imbedded itself in the sharp pycnocline, the desired position. In the event either of the former motions occurred, benzene or carbon tetrachloride, as appropriate, was added to alter the solution density; and another trial particle was injected into the layered system. Usually, one admixture was required to obtain the proper density. Because of the initial near-homogeneity of the two layers, attempts to suspend a particle near the mid-depth of each layer were unsuccessful.

Methyl violet dye was mixed into some of the particle solution and proved to be an aid in tracking an individual particle, particularly in the lower dyed, translucent layer. The undyed-particle solution was satisfactory for particles just above the pycnocline.

3.8 Photographic Data Extraction and Analysis.

Wave and particle motion was photographed with a 16 mm motion picture camera at the rate of eight exposures per second. Kodak black-and-white, plus-X reversal film was used and proved satisfactory. All motion was photographed through an acetate grid, on which lines were spaced at 2 cm, taped to the front of the tank. A stopwatch was placed on the grid

field to provide a time reference. All photography was accomplished with the camera approximately one meter from the side of the tank, with top lighting to provide sufficient differential refraction through the particles for identification. Best results were obtained with a white background approximately 25 cm on the other side of the tank.

Analysis was accomplished by projecting the film with a motion picture projector onto graph paper. The graph paper was aligned parallel to the projected grid, and the 2 cm grid reference marks were drawn on the graph paper. Limitations of the projection equipment did not allow frame-by-frame viewing. The time interval between frames examined was approximately one-half second. The particle position was marked on the graph paper with an appropriate time mark for successive positions. In this manner particle trajectories were obtained.

Wave lengths were obtained in a similar manner by tracing the color discontinuity which occurred at the interface on the graph paper and measuring the distance between appropriate wave phases. The stopwatch readily provided the time interval required for computing phase velocities.

4. INTERNAL WAVE THEORY.

4.1 A Two-layer Model.

Internal waves may exist in any stratisfied fluid (Defant [2]). In a two-layer system, maximum particle motion occurs at the internal boundary surface. Defant further shows that the ratio of the surface wave amplitude to internal wave amplitude is $\Delta\rho/\rho_1$, where $\Delta\rho$ is the density difference between the two layers and ρ_1 is the density of the bottom layer. The phase velocities for the surface wave and the internal wave of a two-layer system are given by

$$c_1^2 = \frac{g}{k} \tanh\ k(h+h') \tag{1}$$

$$c_2^2 = \frac{g}{k} \frac{\rho - \rho'}{\rho \coth kh + \rho' \coth kh'} \tag{2}$$

4.2 Generation.

Rattray [3] has developed a theory which shows that internal waves may be generated by the surface tidal current or wave impinging on a continental shelf. Weigand's [4] model-tank study at the University of Washington has supported the theory. As early as 1912, Zeilon [5] developed a theory and obtained qualitative model-tank results wherein an internal wave could be generated by a current passing over a submarine ridge. Proudman [6] provides a mathematical treatment of internal wave generation by a current flowing over a ridge.

5. GENERAL EXPERIMENTAL PROCEDURES.

Several hours prior to conducting an experiment, water was drawn into the tank and the vat in which the brine was to be mixed. About one hour was required to dissolve sufficient rock salt to yield salinities of 20 to 35 parts per thousand and to allow equilibrium temperature to be reached. After the brine was formed, the Rhodamine "B" dye was added and thoroughly mixed. The brine was siphoned after the fresh water in the tank had drained to the approximate depth desired for the upper layer. A check on the rate of mixing at the interface was made by observing the diminution of the vertical extent of the clear layer, and the rate of siphoning could be adjusted to keep mixing at a minimum. After termination of the siphoning, the water was sampled to determine the vertical density distribution. Sample depths were selected about 1 cm above and below the apparent pycnocline and at intervals of 2 to 3 cm thereafter. The dyed particles were then introduced. They were placed along the centerline of the tank between the absorber and ridge at intervals of approximately 2 to 5 cm. This particle interval was sufficiently large to permit particle discrimination, yet small enough to show the interaction between particles.

When the lighting and camera were in position, the wave generator was activated. During the first two cycles the period of the generator was precisely adjusted to that desired for the experiment. This was necessary since the period of rotation of the generator varied up to three seconds during initial strokes. The generator was then timed for 10 cycles and from this figure the average period of the stroke determined.

6. RESULTS.

6.1 Capabilities and Limitations of the Installation.

Progressive and standing internal waves were generated in an approximate two-layer system by generating an oscillating current over a submarine barrier. Introduced as controlled variables were the generator period, height and form of the barrier, and the depth and density of the two layers. The wave absorber was removed for Run 4A to determine the standing wave characteristics of the basin.

The generator was operated at periods ranging from 5 seconds to 23 seconds. The period of the drive system tended to decrease during the running of an experiment. The change in period was more pronounced at high periods, where the maximum observed change in period was 2 seconds from the beginning to the end of an experiment of 12 minutes' duration. Near the low period range, the deviation was approximately one-half second.

The "flow-by" around the generator plate, which was previously described, continued throughout the course of this investigation. Visual observation of the basin between the barrier and the generator disclosed the presence of eddies, particularly near the bottom of the generator plate, apparently a result of relatively high velocity "flow-by" which occurred on the backstroke. These eddies did not appear to contribute significantly to water motion in the region of the tank where the wave data were taken.

Of the two types of submarine models evaluated, viz., the vertical plate and the sheetmetal form, the latter provided more satisfactory results. Eddies in the vicinity of this formed barrier were minimized, and at large generator periods, eddies were not observed. The major

difficulty encountered in the use of the sheetmetal barrier was that prefabrication and subsequent assembly within the tank were required. This was due to structural members along the top of the tank which provided an access width 10 cm less than the required width of the model. The design adopted for use in the tank is shown in fig. 6. Plastic tape placed around the edges of the model provided the required seal against water seepage around and under the model.

An additional difficulty was encountered in that simultaneous siphoning into both basins was required when the sheetmetal model was used since insertion of the model required a dry tank. During the siphoning it was important to increase the bottom layer depths at the same rate in order to prevent a current between the basins at the interface. When the plate barrier was used, siphoning of the entire layer could be effected with subsequent insertion of the barrier.

An approximate two-layer system was effectively formed for all the experiments. A typical profile of salinity and density is given in fig. 8. The vertical profiles readily provided the respective layer depths and densities.

Mixing at the interface rapidly destroyed the sharp pycnocline as shown in fig. 8. The degeneration of the two-layer system was additionally recognizable in that, after approximately 2 to 3 minutes of wave action, changes in wave length were observed indicating oscillations of other modes. Due to the mixing, the system after 3 minutes is considered to be a poor approximation of a two-layer system. It is noteworthy that mixing at the interface caused an increase in salinity in the upper layer, although a corresponding color gradient in the upper layer was imperceptible to the author. It would appear that a threshold of color response

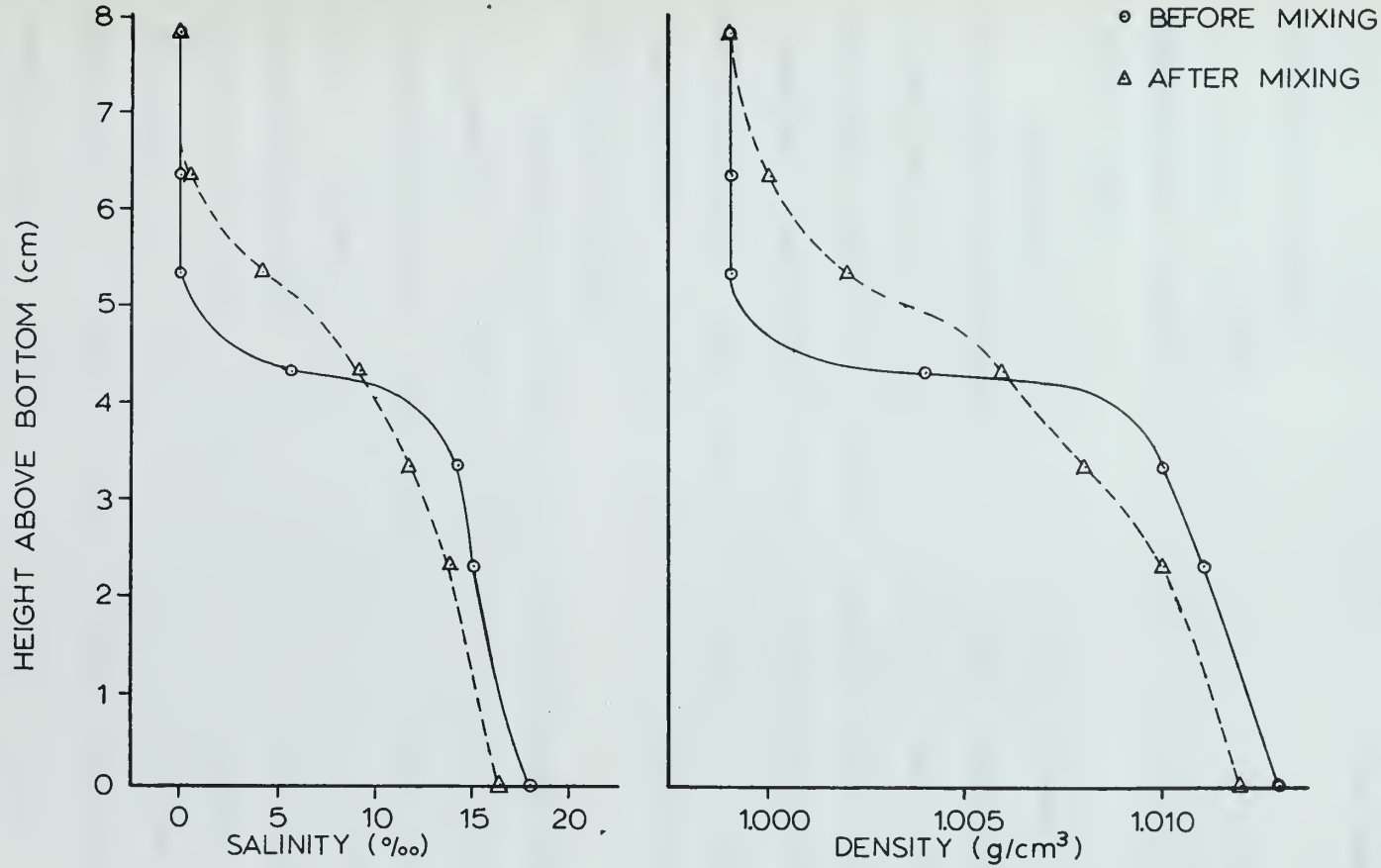

TYPICAL DISTRIBUTIONS of SALINITY and DENSITY

FIGURE 8

of the human eye to the Rhodamine "B" dye tends to generate an apparent discontinuity in the vertical dye distribution. Despite this particular characteristic of the dye, the technique of utilizing a dyed layer contributed significantly to the determination of the internal wave form.

6.2 Data Evaluation.

Data were obtained from 600 ft of film which was used to photograph approximately 45 minutes of wave motion. A data summary is given in Tables 1 and 2.

A qualitative analysis of the data was performed in order to determine some of the characteristics of internal waves which were generated by the flow over the barrier. Two methods of analysis were conducted. One method consisted of tracking a neutrally buoyant particle at the interface at approximately one-half second intervals and plotting a particle trajectory. The second method consisted of tracking the crests of the internal waves and determining the wavelengths, periods, amplitudes and phase velocities.

The objective of the particle analysis was to determine particle trajectories. A particle trajectory over a period of 64 seconds was determined in Run 2A. The trajectory for the first 32 seconds is given in fig. 9. During the period of observation, the internal waves were progressing from right to left. Except for two small-diameter orbits, all orbits had a counter-clockwise direction of rotation, as would be expected from theory for a particle in the lower layer near the interface. With data from fig. 9, graphs of vertical and horizontal particle displacement versus time were obtained as shown in figs. 10 and 11. Analysis of fig. 10 disclosed that the vertical particle motion appeared to have a periodicity which consisted of two periods of approximately five seconds and

Run	1A	1B	1C	2A	3A
h' (cm)	0	7.2	7.6	7.1	6.9
h (cm)	15.2	8.0	8.5	8.1	9.0
$h + h'$ (cm)	15.2	15.2	15.2	15.2	15.9
T_o (sec)	23.0	21.0	21.0	6.0	13.0
T_{is} (sec)			26.3	9.6	4.0
T_{ip} (sec)			5.0	4.9	6.3
L_o (cm)	5.1	5.1	5.1	5.1	5.1
L_{ip} (cm)			22.0	16.0	17.0
H_i (cm)		0.8	1.2	1.8	1.0
ρ' (g/cm^3)		0.999	0.999	0.999	0.999
ρ (g/cm^3)	0.999	1.025	1.024	1.022	1.017
$\Delta\rho$ (g/cm^3)		0.026	0.025	0.023	0.018
t_w (^oF)	61	63	63	62	61
h_B (cm)	7.6	2.5	7.6	7.5	7.5
L_1 (cm)	136	136	136	85	85
L_2 (cm)	160	160	160	193	193
C_{io} (cm/sec)		6.8	5.0	3.3	2.7
C_{it} (cm/sec)			6.4	5.3	4.8

DATA SUMMARY

TABLE 1

Run	4A	5A	6A	6B	7C
h' (cm)	6.9	7.8	3.8	3.3	3.8
h (cm)	9.0	4.0	3.5	4.0	4.0
$h + h'$ (cm)	15.9	11.8	7.3	7.3	7.8
T_o (sec)	12.0	10.0	5.0	8.0	12.6
T_{is} (sec)	6.8	9.0	5.0	10.0	
T_{ip} (sec)	5.1	13.0	5.0	7.0	6.3
L_o (cm)	5.1	5.1	5.1	5.1	5.1
L_{ip} (cm)		34.0	30.0	40.0	21.0
L_{is} (cm)	26.2				
H_i (cm)	2.7	1.5	1.3	1.0	1.0
ρ' (g/cm^3)	1.007	0.999	0.999		0.999
ρ (g/cm^3)	1.014	1.021	1.020		1.011
$\Delta\rho$ (g/cm^3)	0.007	0.022	0.021		0.012
t_w (^oF)	59.5	62	62	62	65
h_B (cm)	7.5	7.5	3.0	3.0	3.0
L_1 (cm)	85	85	88	88	88
L_2 (cm)	196	193	199	199	199
C_{io} (cm/sec)		2.6	6.0	5.7	3.4
C_{it} (cm/sec)		8.2	5.6		4.0

DATA SUMMARY

TABLE 2

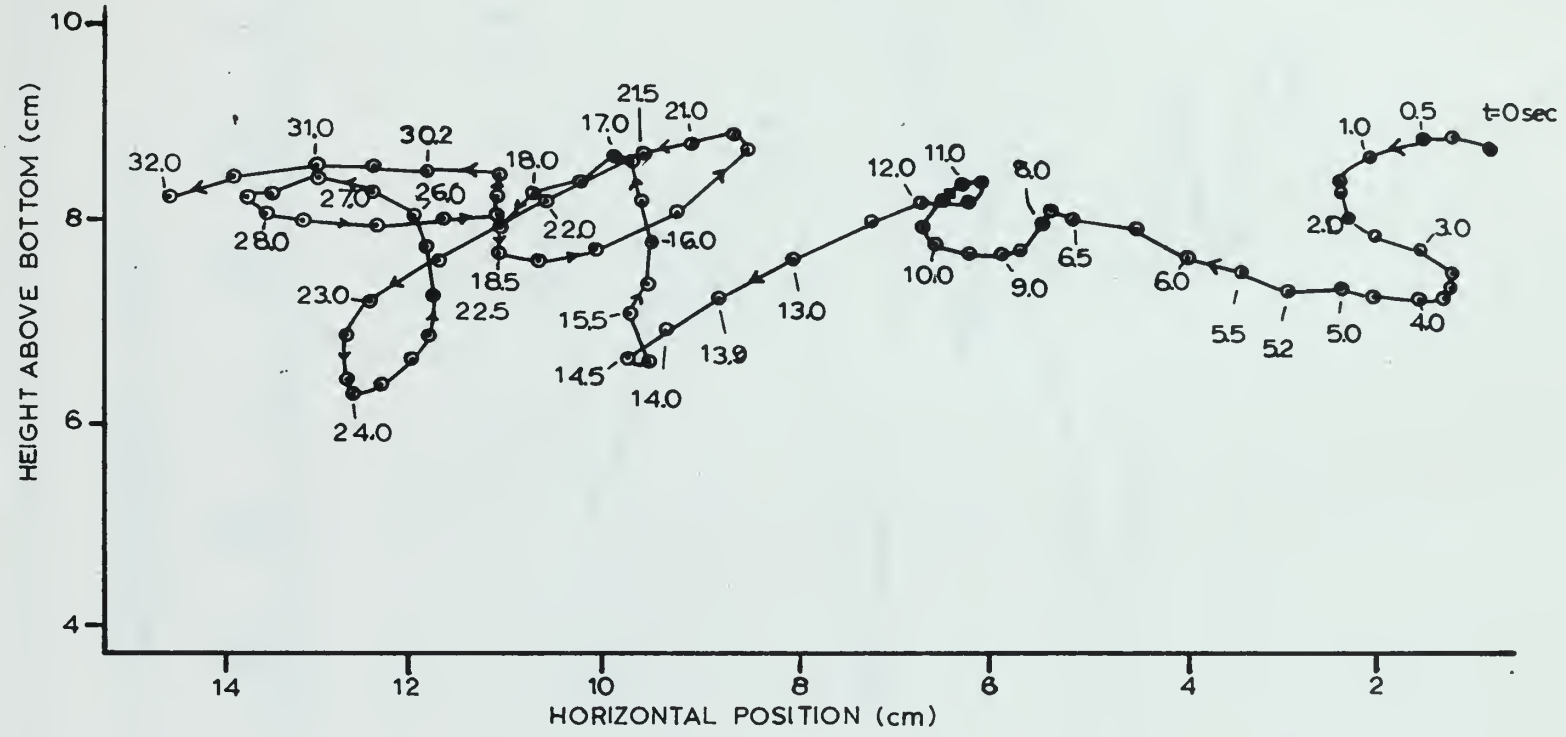

PARTICLE TRAJECTORY

FIGURE 9

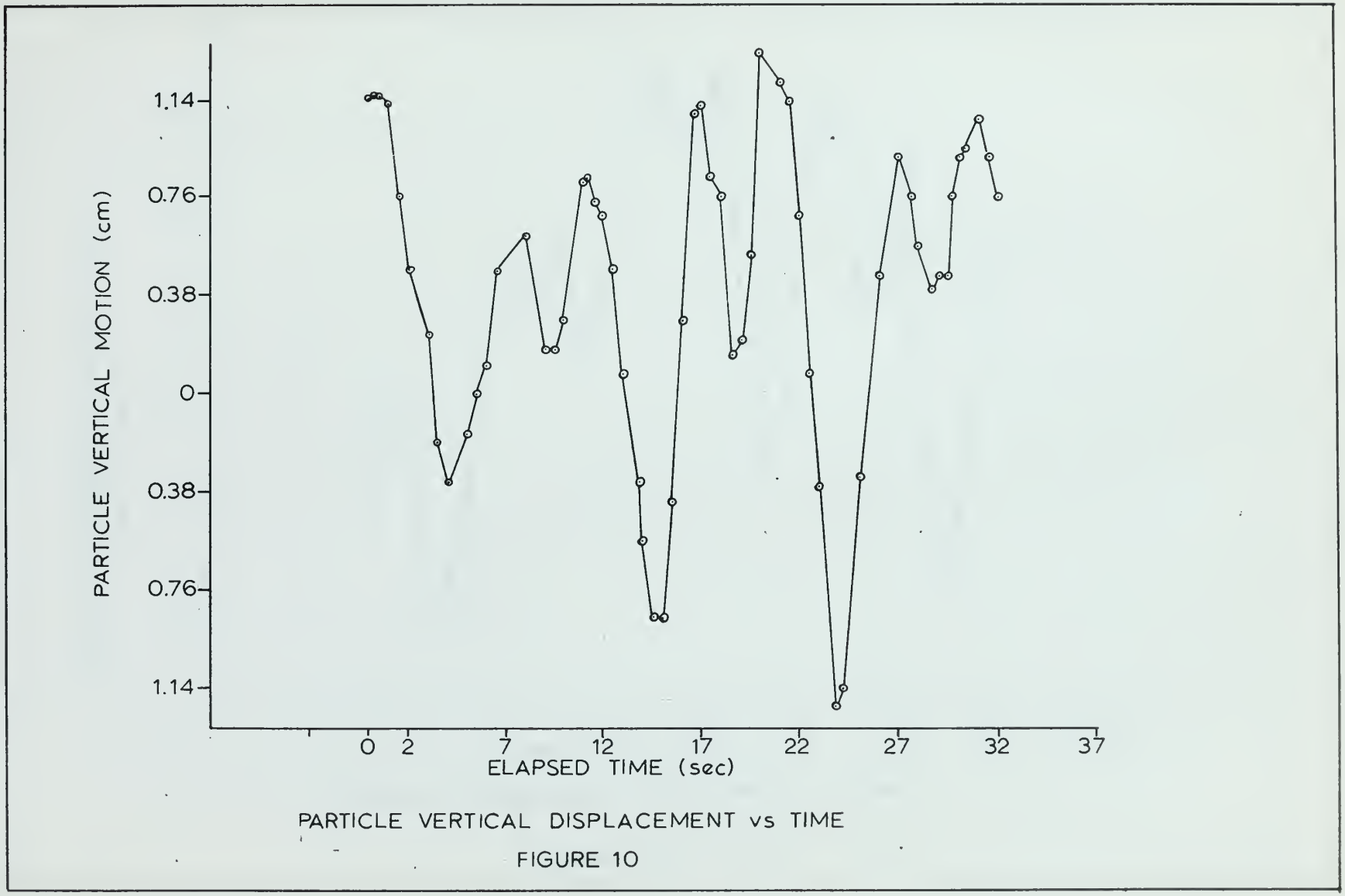

PARTICLE VERTICAL DISPLACEMENT vs TIME

FIGURE 10

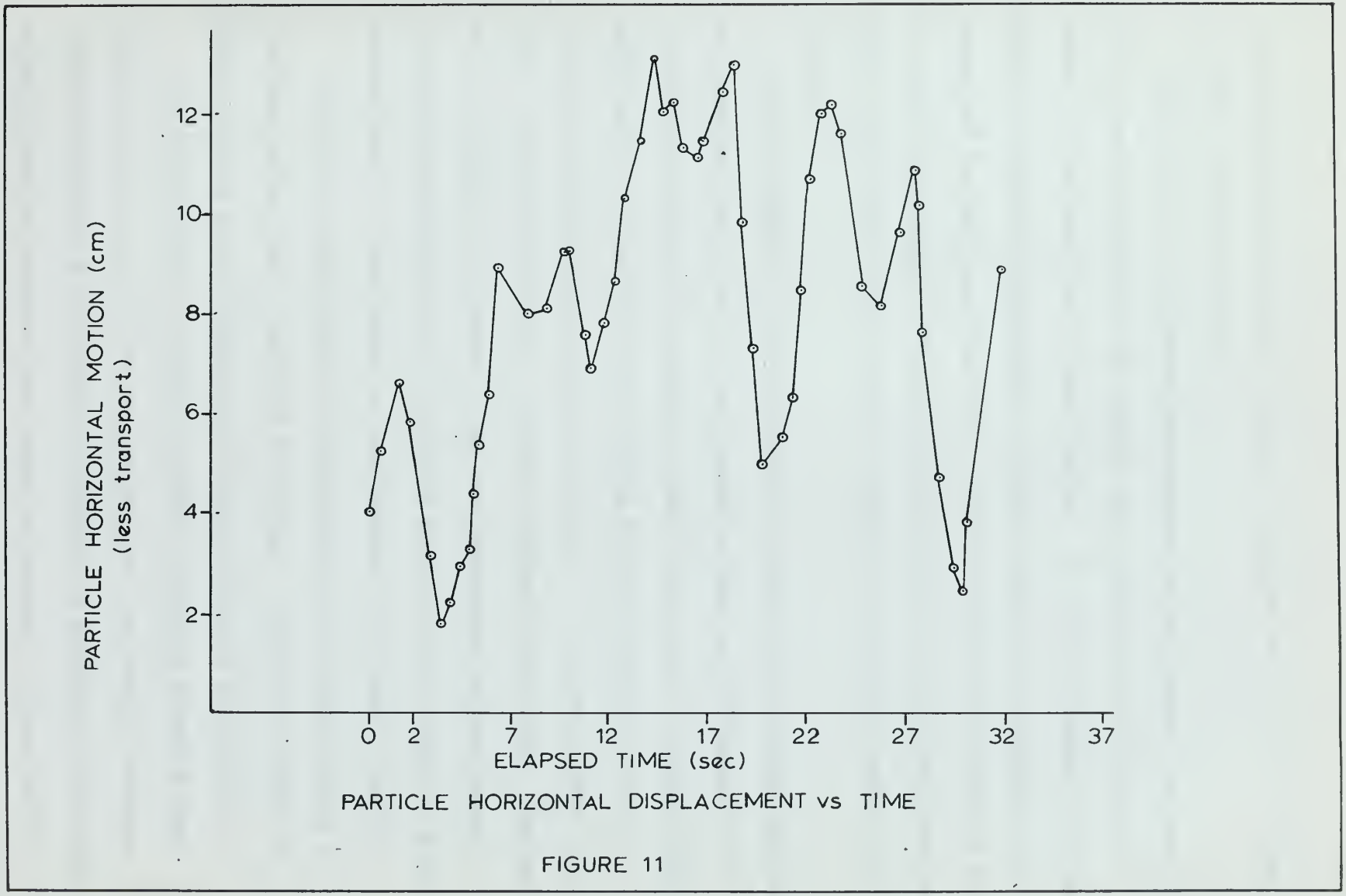

PARTICLE HORIZONTAL DISPLACEMENT vs TIME

FIGURE 11

ten seconds, respectively, and in phase at the time the particle attained its lowest vertical position.

The analysis of horizontal displacement versus elapsed time shown in fig. 10 was complicated by an apparent mass transport of 23.3 cm in 64 seconds in the direction of wave progress. In order to examine only the periodic horizontal displacement, the mass transport was assumed to be linear; and for each data point the transport distance was subtracted from the total displacement. The resultant periodicity of horizontal particle motion shown in fig. 11 is similar to that for the vertical motion shown in fig. 10.

For the segment of time for which the above particle motion analysis was conducted, the period of the progressive wave was determined to be 4.9 seconds by timing the movement of wave crests past a reference mark. Additionally, the period of the standing wave was observed to be 9.6 seconds by timing the horizontal oscillations of a column of water between a surface particle and a particle resting on the bottom. The periods of oscillation determined by the two independent methods compare favorably and indicate that the particle motion was the result of a progressive wave in a mass which was oscillating with a greater period.

The item of significance of this segment of the investigation is that some success was achieved in developing a technique by which the particle motion of an internal wave could be observed and analyzed.

The second method of analysis involved comparing observed phase velocities with those for the theoretical two-layer model. The wave characteristics which were directly observed, in addition to the phase velocity, were the apparent wave length and period. A phase velocity was computed from the apparent wave length and period using the relationship

$$C = L/T \qquad (3)$$

and compared with that phase velocity which was directly observed. The determination of the observed phase velocity by two methods provided a check against inaccuracies of observation. The observed phase velocities determined by the two methods, for any given run, differed by less than 10 percent. The average value of the two observed phase velocities is shown in Tables 1 and 2.

The theoretical phase velocities were computed using equation (2). Within the range of variables introduced, equation (2) shows that the phase velocity of the internal wave is most responsive to changes in the density difference between the two layers. Comparison of the observed and theoretical phase velocities shown in Tables 1 and 2 indicates a maximum difference between the two equal to 44 percent of the theoretical value. Considered significant, however, is the fact that for Runs 1C, 2A, and 3A the magnitude of the observed phase velocities decreases with a decreasing density difference, which is what would be expected from theoretical considerations. A similar trend is observed between Runs 6A and 7A. The discrepancies between the theoretical and observed phase velocities may be a result of the observation of "apparent" phase velocities in a dispersive medium. In all cases conditions were such that the waves are not long; since more than a single frequency is present, there is dispersion and the crests cannot be expected to be conserved. Additional factors which may contribute to the discrepancies are that the progressive wave crest which was observed was superimposed on a standing wave of higher period and that the physical system deviates from the two-layer model.

7. CONCLUSIONS.

In an approximate two-layer system, an internal wave may be generated by a current flowing over a submarine ridge where the height of the ridge may be greater than, less than or equal to the depth of lower layer.

The theory that the phase velocity of an internal wave is directly proportional to the density difference of a two-layer system has been qualitatively supported.

Particle trajectories as predicted by theory may be observed by using neutrally buoyant particles of carbon tetrachloride and benzene.

BIBLIOGRAPHY

1. Cromwell, T. Pycnoclines created by mixing in an aquarium tank. Journal of Marine Research, v. 18, no. 2, 1960: 73-82.

2. Defant, A. Physical Oceanography, v. 2, Pergamon Press, New York, 1961: 517-570.

3. Rattray, M. On the coastal generation of internal tides. Tellus XII, 1960: 54-62.

4. Weigand, J. G. A Model Study of Internal Waves, Thesis, University of Washington, 1962.

5. _____. H.O. Misc. 15360, Effects of Weather Upon the Thermal Structure of the Ocean. U. S. Navy Hydrographic Office: 36-37.

6. Proudman, J. Dynamical Oceanography, Methuen and Co. Ltd., London, 1953: 349-351.